Sexually antagonistic coevolution between the sex chromosomes of *Drosophila melanogaster*

Katrine K. Lund-Hansen[1,2*+], Colin Olito[1+], Edward H. Morrow[2], & Jessica K. Abbott[1]

[1] Department of Biology, Section for Evolutionary Ecology, Lund University, Lund 223 62, Sweden.
[2] School of Life Sciences, University of Sussex, Brighton BN1 9QG, United Kingdom
[*] Corresponding author e-mail: Katrine.Lund-Hansen@biol.lu.se
[+] Equal contributions

Manuscript elements: Table 1, Figure 1, Figure 2, Figure 3, Figure 4; Online Supplementary Material: Appendix A – Empirical methods: Figure S1, Table S1, Table S2, Table S3, Table S4; Appendix B – Development of the recursions.

Running Head: Coevolution between the sex chromosomes

Keywords: Coevolution; Compensatory evolution; Interlocus sexual conflict; Sex chromosome evolution; Sperm Competition; Egg-to-adult survival.

Abstract

Antagonistic interactions between the sexes are important drivers of evolutionary divergence. Interlocus sexual conflict is generally theorised as a conflict between alleles at two interacting loci whose identity and genomic location are arbitrary. Here we build on previous theory and suggest that when these two loci are located on the X and Y (or Z and W) chromosomes, it can lead to cycles of antagonistic coevolution between the sex chromosomes and the two sexes. To test this hypothesis, we performed experimental crosses using *Drosophila melanogaster* where we reciprocally exchanged the sex chromosomes between five wild-type populations in a round-robin design. Disrupting putatively coevolved sex chromosome pairs resulted in increased male reproductive success in 16 out of 20 experimental populations (10 of which were significant), but also resulted in lower offspring egg-to-adult viability that affected both male and female fitness. However, after 25 generations of experimental evolution these sexually antagonistic fitness effects appeared to have been resolved. To help formalise our hypothesis, we developed population genetic models of antagonistic coevolution using fitness expressions based on our empirical results. Our models support the conclusion that antagonistic coevolution between the sex chromosomes is plausible under the fitness effects observed in our experiments. Together, our results lend both empirical and theoretical support to the idea that a cycle of antagonistic coevolution can occur between sex chromosomes, and illustrates how this process may drive genetic and phenotypic divergence between populations.

Introduction

Sex chromosomes have a number of unique features distinguishing them from the rest of the nuclear genome and giving them particular importance in evolutionary biology. The sex chromosomes differ both from the autosomes, and from one another, in their mode of inheritance, the selection experienced in the two sexes, and gene content (1). Moreover, these processes are interdependent and strongly influence the genetic variation harboured on each chromosome. The Y (or W) chromosome is inherited only through the heterogametic sex (XY/ZW), whereas the X (or Z) chromosome is inherited from both the hetero- and homogametic (XX/ZZ) sex (1). The Y chromosome will therefore only experience selection in males, but the X chromosome, which spends two-thirds of its time in females, will regularly experience selection in females (1). However, the X chromosome is hemizygous in males and will therefore also always be exposed to selection when present in males (i.e., X-linked genes are unsheltered by dominance effects in males) (2). Though the X chromosome is shared by the sexes, the X chromosome in *Drosophila melanogaster* has been shown to harbour more female-biased than male-biased genetic variation (3, 4), whereas the Y chromosome has been shown to impact male fitness traits (5–7).

These unique properties of the sex chromosomes give them an important role in two major fields within evolutionary biology: speciation (8) and sexual conflict (1, 9). Here we aimed to investigate whether interactions between sex chromosomes contribute to between-population divergence at the intra-specific level. To do so we performed experimental crosses to 'swap' either an X or a Y chromosome between five populations of *D. melanogaster*, allowing us to isolate the effects of novel interactions between the sex chromosomes on male reproductive fitness. As we outline below, we expected to see different patterns of male reproductive success depending on whether population divergence is caused by the accumulation of sex-linked sterility mutations (or other incompatibilities contributing to reproductive isolation between populations), or is instead a result of sexually antagonistic coevolution between the sex chromosomes.

If interactions between the sex chromosomes contribute to divergence between these populations primarily through accumulation of X-linked incompatibilities, we would expect to see a decrease in male fitness in the experimental populations as

these incompatibilities are exposed to selection in males. The X chromosome has a large effect on hybrid male sterility (10), and the accumulation of incipient 'hybrid incompatibilities' begin in allopatric populations within a species prior to speciation (11). However, while previous studies have found evidence of early prezygotic isolation between sub-Saharan and cosmopolitan populations of *D. melanogaster* (12, 13), there is limited evidence for postzygotic isolation (14). On the other hand, sexual conflict between the sex chromosomes could, in principle, provide an alternative mechanism for them to contribute to evolutionary divergence between populations (15), as Y-linked regulation of gene expression has been indicated to do (16).

Sexually antagonistic coevolution is based on the Red-Queen process among species playing out between the sexes (17). Simply put, sexually antagonistic coevolution describes an antagonistic interaction between the sexes in which males increase their reproductive success through an adaptation that is simultaneously detrimental to females, which creates selection for counter-adaptation in females to regain their lost fitness; the process may be repeated in multiple cycles over evolutionary time until a resolution is reached or a palliative adaptation ends the conflict (18). Sexually antagonistic coevolution is a form of interlocus sexual conflict (15) if the traits involved are encoded by different genes in males and females (19). As first proposed by Rice & Holland in 1997, when the loci in question are located on the sex chromosomes, this could lead to cycles of sexual antagonistic coevolution between the sex chromosomes (15). If a Y-linked male-beneficial mutation arises that increases male reproductive success but decreases female fitness, it should spread through a population because it is subject to selection in males only. We might then expect selection for any compensatory mutation that might arise on the X chromosome or autosomes to increase female fitness again. Such mutations will likely differ between allopatric populations, and we would therefore expect to find an increase in male reproductive fitness when a Y chromosome with male beneficial mutations is paired with an X chromosome without the corresponding compensatory mutation(s). According to the sexually antagonistic coevolutionary model, we also predict a decrease in female fitness when mating with males harbouring a Y chromosome in a novel X chromosome background. Another corollary of the antagonistic coevolutionary model is that the effect of disrupting coevolved sex chromosomes on male and female fitness should decay over subsequent generations as new compensatory mutations arise, or novel combinations of segregating alleles

achieve a similar compensatory effect. We tested this prediction by examining male and female fitness in our experimental populations again after 25 generation of experimental evolution. Crucially, the signature of antagonistic coevolution between the sex chromosomes in terms of male and female fitness differs from that for the accumulation of sex-linked incompatibilities, allowing us to identify whether one or other process is driving evolutionary divergence between populations.

To complement our empirical results and help formalize our hypothesis of sexually antagonistic coevolution between the sex chromosomes, we developed population genetic models describing the evolution of two interacting loci located in different genomic regions (i.e., unlinked): a Y-linked locus influencing both adult male fertilization success (i.e., sperm competition) and subsequent offspring survival, and a compensatory locus affecting only offspring survival located on either an autosome or the X chromosome.

Results and Discussion

Empirical Results

To empirically test for evidence of population-specific interactions between the sex chromosomes in *D. melanogaster*, we crossed five outbred laboratory-adapted wild-type populations derived from four continents and three climatic zones in a round robin cross design (Fig. 1). We created 20 novel populations where either the X chromosome (*novel X* treatment) or the Y chromosome (*novel Y* treatment) from one wild-type population (*wt*) was incorporated into another population (*SI Appendix A*, Fig. S1). We found a significant effect of treatment on male relative reproductive fitness (*SI Appendix A*, Table S1), with males from the *novel X* or *novel Y* treatments having a significantly higher relative fitness than *wt* males (Fig. 2*A*, *SI Appendix A*, Table S2). To exclude interactions between the novel sex chromosome and the autosomes, we also created a *novel XY* treatment where a pair of sex chromosomes from one *wt* population were introduced into another population (*SI Appendix A*, Fig. S2). We found no significant effect of treatment on relative fitness in the assay with *novel XY* treatments (Fig. 2*B*, *SI Appendix A*, Table S1). It therefore seems that introducing an individual novel sex chromosome caused the fitness differences rather than the autosomal background. Mitochondria-nuclear interactions have previously been shown to affect male fertility in *D. melanogaster* (20), and both *novel X* and

142 *novel Y* chromosomes were expressed with novel mitochondria. However, the *novel*
143 *XY* chromosomes also were expressed with novel mitochondria and we found no
144 effect on male fitness in these populations, suggesting that the magnitude of any mito-
145 nuclear interactions was minor in these populations compared to the effect of
146 interactions between the sex chromosomes. To investigate the interaction between the
147 sex chromosomes in more detail, we calculated the difference in fitness between the
148 novel populations and their *wt* counterparts (ΔFitness = $\omega_{\text{novel population}} - \omega_{\text{wild-type}}$). We
149 used bootstrap methods to model the data, and found that 10 of the 20 novel
150 populations were significantly different from zero in a positive direction (Fig. 2*C*, *SI*
151 *Appendix A,* Table S3). 16 out of the 20 point estimates were also positive, which is
152 significantly different from what would be expected under random deviations (P =
153 0.01). Taken together, our results demonstrate that exchanging a sex chromosome
154 between populations of *D. melanogaster* had a positive overall effect on male fitness.
155 This was consistent with the expected signature of antagonistic coevolution between
156 the sex chromosomes on male fitness, but not with that of accumulated sex-linked
157 incompatibilities influencing male sterility.

158 To tease apart which fitness components were driving the overall pattern of
159 increased relative fitness in the *novel* populations, we looked at a number of
160 phenotypic traits that are correlated to male fitness. Interestingly, we found that the
161 increase in fitness was related to different traits in the two *novel* sex chromosome
162 treatments. For *novel X* males, we found that the increase in fitness was correlated
163 with an increase in size, as *novel X* males were significantly larger than both *wt* and
164 *novel Y* males (*SI Appendix A,* Fig. S3*A*, Table S1 & S2). Body size is an important
165 factor in male fitness (21), and larger males have been shown to have a mating
166 advantage (22). For *novel Y* males we found that the increase in fitness was correlated
167 with an increased ability to displace other males' sperm (*SI Appendix A*, Fig. S3*B*,
168 Table S1), as *novel Y* males were significantly better at displacing sperm compared to
169 *wt* males (*SI Appendix A,* Table S2). It therefore seemed that the *novel X* males gained
170 a mating advantage from an increase in size, whereas the *novel Y* males gained the
171 advantage through being better at sperm displacement. Thus, the results suggest that
172 different phenotypic and genetic mechanisms may be responsible for the increased
173 male fitness observed in the two *novel* sex chromosome treatments.

174 If the coevolution between the sex chromosomes is antagonistic in nature, the
175 increase in male fitness should come at a cost to female fitness. We found a
176 significant effect of treatment on total offspring number (*SI Appendix A*, Fig. S4*A*,
177 Table S1), with *novel X* males siring a lower number of live offspring compared to *wt*
178 males (Table S2). However, we did not find any difference in number of eggs laid by
179 females mated with males from the different treatments (*SI Appendix A*, Fig. S4*B*,
180 Table S1). The discrepancy between number of eggs and live offspring suggest a
181 trade-off between number of offspring and offspring quality, which was confirmed by
182 a significant difference in egg-to-adult viability (SI Appendix A, Fig. S4*C*, Table S1).
183 *Novel X* males sired significantly lower numbers of viable offspring than the other
184 two treatments (*SI appendix A*, Table S2). So mating with *novel X* males decrease a
185 female's fitness by reducing the overall number of live offspring she produces. A
186 decrease in offspring survival could be caused by meiotic drives seen in a departure
187 from 50:50 sex ratio (23). We did not find a significant difference in sex ratio between
188 the different treatments (*SI Appendix A*, Fig. S4*D*, Table S1). There are also no known
189 sex ratio meiotic drivers in *D. melanogaster*, so the decrease in offspring survival was
190 most likely caused by the father's genotype. We were unable to establish which
191 harmful effects *novel Y* males had on female fitness through the assays performed in
192 this experiment. But we were able to exclude increased male harassment (e.g. due to
193 larger size), males inducing high fecundity, and reducing offspring viability. A
194 possible cause to investigate in the future is the reduction of female receptivity after
195 mating with males, which could lead to a reduction in female lifetime reproductive
196 fitness.
197 If the sex chromosomes coevolve antagonistically any shift towards increased
198 fitness in one sex at the cost of the other sex could lead to counter-adaption, which we
199 expected to see as a reduction in male fitness over time. In principle, this subsequent
200 reduction in male fitness could be due to new X-linked compensatory mutations;
201 however, given the time-scale of the experiment it is more likely that any
202 compensatory evolution by females must utilize standing genetic variation in the
203 stock populations, with novel allelic combinations achieving a compensatory effect.
204 After 25 generations of experimental evolution (*SI Appendix A,* Fig. S5), we repeated
205 both the male reproductive fitness assay and two of the significant phenotype assays
206 to test if the interactions between the novel pairs of sex chromosomes had changed.
207 As predicted, we no longer found a significant treatment effect on male fitness (Fig.

3*A*, *SI Appendix A,* Table S4). Indeed, we found that ΔFitness (ΔFitness = $\omega_{\text{novel population}} - \omega_{\text{wild-type}}$) between novel populations and their wild-type counterparts had diminished in magnitude and were no longer significantly different from 0 (except for one population, I–O_X) (Fig. 3*B*, *SI Appendix A,* Table S5). The reduction in fitness observed after just 25 generations indicates a strong selection pressure for compensatory evolution, which is supported by the simulation results. We also no longer found an effect of the treatments on sperm competition (*SI Appendix A,* Fig. S6*A*, Table S4) or offspring egg-adult survival (*SI Appendix A,* Fig. S6*B*, Table S4). There was a significant effect of the treatments on sex ratio (*SI Appendix A,* Fig. S6*C*, Table S4) as *novel Y* males produced significantly more male offspring than *wt* males (*SI Appendix A,* Table S6). However, this significant difference was not due to a change in sex ratio in the *novel Y* populations; rather it was due to a change in the sex ratio in the *wt* populations.

Taken together, our empirical results are consistent with predictions for antagonistic coevolution between the sex chromosomes. To further validate that we found evidence of antagonistic coevolution, we built a theoretical model based on our empirical evidence.

Theoretical Models

Consider two alternative genetic systems involving two unlinked loci: a Y-linked locus (**Y**, with alleles *Y*, and *y*), and a compensatory locus located on either an autosome (**A**, with alleles *A*, and *a*) or the X chromosome (**X**, with alleles *X*, and *x*) (the Autosomal and X-linked models respectively), in a large population with discrete generations. In both models, a mutant *y* chromosome increases male fertilization success by a rate of $1 + s_m$ relative to the wild type (*Y*), but also reduces viability of offspring resulting from matings with females carrying the wild-type allele at the compensatory locus, *A* (or *X*). At the same time, females carrying the mutant *a* (or *x*) compensatory allele may incur a 'cost of compensation' in terms of offspring viability when mating with wild-type (*Y*) males (see Table **1** and Materials and Methods for a summary and description of fitness expressions). These fitness expressions create a scenario of antagonistic coevolution between a potentially male-beneficial Y-linked mutation, and the compensatory locus. Reminiscent of standard theories of compensatory evolution (e.g., (24, 25)), each of the mutant alleles (*y* and either *a* or *x*)

241 reduces offspring survival in isolation. However, unlike previous theory, the two loci
242 are located on different chromosomes that do not recombine with one another; if a
243 mutant *y* chromosome spreads to fixation, compensation at the population level
244 requires that the compensatory mutation also fixes (see also recent models of
245 "Father's Curse" for similar scenarios, but without compensatory evolution or
246 parental effects on offspring viability (26); a full description of the models is
247 presented in the Materials and Methods and in *SI Appendix B*). Our theoretical
248 analyses focus on (i) the evolutionary invasion of rare mutants at each locus
249 individually; and (ii) single bouts of coevolution, beginning with invasion of a single-
250 copy mutant *y* chromosome in a population initially fixed for the wild-type *Y*
251 chromosome and for the wild-type *A* (or *X*) allele at the compensatory locus, and
252 completing when both mutant alleles *y* and *a* (or *x*) become fixed (see (31) for a
253 similar approach in the context of mito-nuclear coevolution).

254 Evolutionary invasion analyses of the two models reveal three key results.
255 Intuitively, invasion of a rare mutant *y* chromosome into a population initially fixed
256 for the wild-type alleles at both loci requires that the increase in fertilization success
257 for mutant males is greater than the accompanying reduction in offspring survival.
258 Neglecting second order terms, a mutant *y* chromosome can spread when $\delta = s_m - s_o >$
259 0. If compensatory evolution is slow relative to the evolution of the Y-linked locus
260 (e.g., the compensatory mutation rate is much smaller than the mutation rate to a
261 mutant *y*), the mutant *y* chromosome is most likely to fix before a new compensatory
262 mutation occurs. In this case, the genomic location of the compensatory locus does
263 not influence the invasion conditions for a compensatory mutation. All males carry
264 the mutant *y*, and so compensatory mutations will spread if there is any selection
265 against the wild-type allele at the compensatory locus (i.e., $0 < h_o, s_o < 1$ for both
266 models). Differences between the models emerge when new compensatory mutations
267 can arise while the mutant *y* chromosome is still segregating in the population. If there
268 is any cost of compensation for females (i.e., $0 < s_c$), compensatory mutations will
269 experience purifying selection while q_y is small because most males carry the wild-
270 type *Y* chromosome. As q_y increases, more matings involve mutant *y* males and
271 females homozygous for the wild-type allele at the compensatory locus. When q_y
272 reaches a threshold frequency, $\tilde{q}_y^A$ ($\tilde{q}_y^X$ for the X-linked model), compensatory
273 mutations will be favoured by selection (derivations provided in *SI Appendix B*). As

illustrated in Fig. 4*A* for the case of additive compensatory fitness effects ($h = h_o = h_c = 1/2$), $\tilde{q}_y^X$ is always less than or equal to $\tilde{q}_y^A$, and the difference between the two thresholds is greatest when $0 < s_o,\ s_c \ll s_m$. Overall, these results suggest that the genomic location of compensatory mutations (Autosomal or X-linked) will be most important when (i) the mutant *y* chromosome is strongly beneficial for males and there is little or no cost of compensation for females (i.e., when $0 < s_o,\ s_c \ll s_m$); and (ii) when compensatory evolution is not limited by mutational variation (i.e., when mutant *y* chromosomes and compensatory mutations are likely to co-segregate in the population). To complement our analytic results, we performed Wright-Fisher simulations to estimate two other important properties of coevolutionary cycles predicted by our models: (i) the probability of invasion of single-copy autosomal (Π_A) and X-linked (Π_X) compensatory mutations into populations of *N* individuals that are initially fixed for the mutant *y* chromosome; and (ii) the total time to complete a single bout of coevolution between the Y-linked and compensatory loci (T_A and T_X, respectively) under recurrent mutation, selection, and drift. Although the invasion conditions for mutant compensatory mutations are the same for both models when the mutant *y* chromosome is initially fixed, the probability of eventual fixation for a single-copy mutation is larger for an X-linked compensatory locus (Π_X) than an autosomal one (Π_A) except for the special case of complete dominance (i.e., when $h_o = 1$) (Fig. 4*B*). The average time to complete a co-evolutionary cycle is also smaller for an X-linked than an autosomal compensatory locus, provided the compensatory mutation rate (μ_a or μ_x) is not dramatically lower than the male-beneficial mutation rate (μ_y) (Fig. 4*C*). When compensatory evolution is strongly limited by mutational variation, compensatory evolution can be faster on the autosomes than the X. This is due to an implicit trade-off between the probability of invasion, which is higher for the X than the autosomes (Fig. 4*B*), and the size of the mutational target, which is lower for the X because males only carry one copy.

Overall, our theoretical results support the conclusion that antagonistic coevolution is (i) plausible under the fitness effects observed in our empirical experiments; and (ii) more likely to involve both sex chromosomes than the Y and an autosome, especially when compensatory dynamics are not slow relative to those of male-beneficial Y-linked mutations. An interesting corollary to these results is that

antagonistic coevolution should drive more rapid among-population divergence on the X chromosome than the autosomes.

Conclusion

In conclusion, we empirically examined the role of the sex chromosomes in evolutionary divergence among allopatric populations of *D. melanogaster*. We found evidence of intragenomic conflict between the sex chromosomes that was independent of any interaction with the autosomes or mitochondria. Disrupting coevolved sex chromosomes resulted in an overall increase in reproductive fitness for *novel* males, through increased body size (for *novel X* males) and sperm displacement (for *novel Y* males), but also decreased offspring egg-to-adult viability. The accompanying reduction in offspring viability created indirect selection on females to mitigate the loss in fitness resulting from mating with a *novel* male. After 25 generations of experimental evolution *novel* males no longer enjoyed higher reproductive fitness and there were no differences in offspring survival, indicating that the sexually antagonistic effects of disrupting coevolved sex chromosomes had been resolved, probably by standing genetic variation for compensatory alleles in the experimental populations. Overall, our empirical results were consistent with a sexually antagonistic coevolutionary model of sex chromosome evolution in allopatric populations. Analysis of our theoretical models supports the plausibility of antagonistic coevolution between the sex chromosomes under the fitness effects observed in the experiments, and predicts that such coadaptation is more likely to involve sex chromosomes than autosomes provided that compensatory evolution is not limited by mutational variation. These new insights into the interactions between the sex chromosomes can help further our understanding of early speciation events. Antagonistic coevolutionary cycles between the sex chromosomes will most likely follow different trajectories in different populations due to random mutations and the interaction between the environment and sexual conflict (27), resulting in genetic and phenotypic divergence between allopatric populations. Thus, over evolutionary time, antagonistic coevolutionary cycles could lead to hybrid incompatibility, and thereby contribute to speciation.

338 # Materials and Methods

339 ## Empirical methods

340 ***Drosophila* husbandry and fly stocks.** We used five outbred laboratory-adapted
341 wild-type populations: (1) *Dahomey*, Africa, tropical (22); (2) *Innisfail*, Oceania,
342 tropical; (3) LH_M, North America, mediterranean; (4) *Odder*, Europa, temperate (29);
343 (5) *Tasmania*, Oceania, temperate. For at least two generations before the cross, we
344 maintained all wild-type populations under the standard LH_M culturing protocol
345 (25°C, 12-12 light-dark cycle, 60% relative humidity, cornmeal-molasses-yeast
346 medium, *SI Appendix A* (28)). For the fitness assays we used an outbred LH_M
347 population homozygous for the visible brown eye (*bw*) genetic marker (LH_M-*bw*).
348
349 **Male reproductive fitness.** We estimated male reproductive fitness as the proportion
350 of live offspring sired by males of the target treatment. Five adult target males were
351 placed in a vial for two days with ten competitor LH_M-*bw* males and 15 virgin LH_M-
352 *bw* females. The females were transferred into a single test tube to oviposit for 18
353 hours after which the females were discarded, and the test tubes left under standard
354 LH_M conditions for 12 days. After which we counted the adult offspring and scored
355 them for eye-colour to assess paternity. The *bw* genetic marker is recessive to the
356 wild-type red eye-colour allele, so all red-eyed offspring can be assigned to red-eyed
357 target males. We calculated relative fitness of the target males by dividing the fitness
358 for each replicate by the maximum fitness across all replicates. We measured male
359 fitness for three different assays: at generation 0 (n = 2 blocks x 7 experimental
360 replicates x 25 populations; fitness estimates for 70 individuals per population), at
361 generation 25 (n = 2 blocks x 3 experimental replicates x 2 replicate populations x 14
362 populations; fitness estimates for 60 individuals per population) and for the sex
363 chromosome-autosome interactions (n = 10 experimental replicates x 10 populations;
364 fitness estimates for 50 individuals per population).
365
366 Construction of the *novel* populations, the evolution experiment, male thorax size,
367 sperm competition assay, male effect on female fecundity, and offspring egg-to-adult
368 viability assay are described in *SI Appendix A*.
369

370 **Statistical procedures**. All the statistical analyses were conducted in R version 3.4.4
371 (30). We fit linear models with treatment as a fixed factor to test each of the
372 dependent variables: thorax size and male effect on female fecundity, and tested for
373 significant effects using ANOVA. We performed post-hoc Tukey HSD comparisons
374 for all analyses with a significant treatment effect. We used linear mixed models
375 (**lme4** (31)) with treatment as a fixed factor and experimental block as a random
376 factor to test the dependent variables: male reproductive fitness, egg-to-adult
377 offspring viability, sex ratio, sperm competition, and total offspring number, and
378 again tested for significant effects using ANOVA. We performed post-hoc Tukey
379 HSD (**multcomp** (32)) comparisons for all analyses with a significant treatment
380 effect. We calculated bootstrap 95% confidence intervals around ΔFitness (ΔFitness =
381 $\omega_{\text{novel population}}$ - $\omega_{\text{wild-type}}$) randomly resampling 13 out of 14 data points and
382 recalculating ΔFitness 10,000 times. We used the Exact Binomial Test to test if there
383 were more positive ΔFitness estimates than expected by chance. For statistical
384 analysis after the 25 generations of experimental evolution we fit linear mixed models
385 with treatment nested within replicate populations to test the dependent variables:
386 male reproductive fitness, egg-to-adult offspring survival, sperm competition and sex
387 ratio. For assays done in experimental blocks, we added experimental block as a
388 random factor, tested for significant effects using ANOVA, and performed post-hoc
389 Tukey HSD tests for analyses with significant treatment effect. We calculated
390 bootstrap 95% confidence intervals around treatment means for ΔFitness by randomly
391 resampling 11 out of 12 data points and recalculating ΔFitness 10,000 times.
392
393 **Theoretical models**
394 We developed two population genetic models, identified by the location of the
395 compensatory locus: the Autosomal and X-linked models respectively. We assumed
396 discrete generations, and a life-cycle that proceeds as follows: (i) birth, (ii) selection
397 on offspring survival, (iii) meiosis and mutation, (iv) selection on male mating
398 success. Both loci in each model are biallelic. The Y-linked locus, **Y**, has wild-type *Y*
399 and mutant *y* alleles with frequencies q_Y and $q_y = 1 - q_Y$. The compensatory locus is
400 denoted **A** (with alleles *A* and *a* and frequencies q_A and $q_a = 1 - q_A$) for the autosomal
401 model, and **X** (with alleles *X* and *x* and frequencies q_X and $q_x = 1 - q_X$) for the X-
402 linked model (wild-type alleles are indicated by capital letters, mutant alleles in

403 lowercase). Following standard population genetics theory, **Y** is effectively haploid
404 with strictly paternal inheritance, while the autosomal or X-linked compensatory loci
405 (**A** or **X**) are diploid with bi-parental inheritance.

406 We based the fitness expressions used in our models loosely on our
407 experimental results. The mutant y chromosome increases male mating success by a
408 factor of $1 + s_m$ relative to the ancestral Y chromosome. Offspring survival depends on
409 the paternal genotype at **Y** and the maternal genotype at the compensatory locus (**A** or
410 **X**), as sires effects offspring viability (33) and any such negative effects should create
411 selection for females to compensate by maternal effects. Offspring sired by mutant y
412 males may experience reduced survival, depending on their mother's genotype at the
413 compensatory locus: matings involving parental genotypes [$y : AA$], [$y : Aa$], and [$y :$
414 aa] result in offspring relative fitness of $1 - s_o$, $1 - h_o s_o$, and 1 respectively. To make
415 the models more general, and analytically tractable, we allowed females carrying the
416 mutant a allele to incur a 'cost of compensation' when mating with wild-type (Y)
417 males: matings involving parental genotypes [$Y : AA$], [$Y : Aa$], and [$Y : aa$] result in
418 relative offspring fitnesses of 1, $1 - h_c s_c$, and $1 - s_c$ respectively (Table **1**). Similar to
419 standard theories of compensatory evolution (e.g., (24, 25)) each of the mutant alleles
420 (y and either a or x) is deleterious in isolation. In our models, however, compensation
421 requires that both parents have the appropriate mutant genotype at the other locus.

422 We model evolutionary invasion and single co-evolutionary cycles between
423 the male-beneficial Y-linked locus and the compensatory locus (see (34) for a similar
424 approach in the context of mito-nuclear coevolution). A bout of coevolution begins
425 with the invasion of a single-copy mutant y chromosome in a population initially
426 fixed for the wild-type A (or X) allele at the compensatory locus. The mutant y
427 evolves under net positive selection if the increase in male mating success outweighs
428 the reduction in offspring survival (i.e., if $\delta = (s_m - s_o) > 0$) until it becomes fixed (q_y
429 $= 1$) or is lost from the population ($q_y = 0$). The compensatory locus (**A** or **X**) evolves
430 under recurrent mutation and selection, with the population initially fixed for the wild
431 type A allele ($q_a = 1$ for the autosomal model) or X ($q_x = 1$ for the X-linked model).
432 For simplicity we assume one-way mutation from $A \rightarrow a$ at a rate u_a, and $X \rightarrow x$ at a
433 rate u_x per meiosis. If females experience a 'cost of compensation' (i.e., when $s_c > 0$),
434 the mutant compensatory locus will evolve under purifying selection until the mutant
435 y chromosome reaches a threshold frequency, denoted $\tilde{q}_y^A$ and $\tilde{q}_y^X$, at which y becomes

selectively favoured. A co-evolutionary cycle completes when the mutant allele becomes fixed at both loci (i.e., $q_y = q_a = 1$ or $q_y = q_x = 1$).

Our analytic results all assume large population sizes (negligible drift), and an equal sex ratio. To identify the conditions under which rare mutant alleles at each locus can spread during key points of an coevolutionary cycle, we performed a linear stability analysis for each model under three different scenarios: (i) invasion of mutant a y chromosome into populations initially fixed for the wild-type allele at both loci (initial frequencies of $q_y = 0$, and $q_i = 0$; where $i \in \{a, x\}$); (ii) invasion of a rare mutant compensatory allele into a population fixed for y ($q_y = 1$, and $q_i = 0$); and (iii) invasion of a mutant compensatory allele into a population with an arbitrary initial frequency of y ($q_y = q_y$, $q_i = 0$). Mutant alleles can invade (i.e., the initial equilibrium is unstable) when the leading eigenvalue of the Jacobian of the system of recursions is greater than one ($\lambda_L > 1$; 43). When the initial frequency of y is arbitrary, solving the expression $\lambda_L > 1$ for q_y yields the threshold frequency at which compensatory mutations become selectively favoured, ($\tilde{q}_y^A$ or $\tilde{q}_y^X$). A full derivation of all models and analytic results is provided in *SI Appendix B*.

We complemented our analytic results with stochastic Wright-Fisher simulations for the Autosomal and X-linked models with population size N and an equal sex ratio. We estimated two important properties of co-evolutionary cycles from the simulations: (i) the probability of invasion of single copy autosomal (Π_A) and X-linked (Π_X) compensatory mutations into populations initially fixed for the mutant y chromosome; and (ii) the total time required to complete a single bout of coevolution between the Y-linked and compensatory loci (T_A and T_X for the autosomal and X-linked models respectively) under recurrent mutation, selection, and drift. Additional details and R code for the simulations can be found in *SI Appendix B*, and online at https://github.com/colin-olito/sexChromCoAdapt.

References

1. J. E. Mank, Small but mighty: the evolutionary dynamics of W and Y sex chromosomes. *Chromosome Res.* **20**, 21–33 (2012).

2. B. Vicoso, B. Charlesworth, Evolution on the X chromosome: unusual patterns and processes. *Nat. Rev. Genet.* **7**, 645–653 (2006).

3. M. Parisi, *et al.*, Paucity of Genes on the Drosophila X Chromosome Showing Male-Biased Expression. *Science* **299**, 697–700 (2003).

4. J. M. Ranz, C. I. Castillo-Davis, C. D. Meiklejohn, D. L. Hartl, Sex-Dependent Gene Expression and Evolution of the Drosophila Transcriptome. *Science* **300**, 1742–1745 (2003).

5. A. K. Chippindale, W. R. Rice, Y chromosome polymorphism is a strong determinant of male fitness in Drosophila melanogaster. *Proc. Natl. Acad. Sci.* **98**, 5677–5682 (2001).

6. C. Rohmer, J. R. David, B. Moreteau, D. Joly, Heat induced male sterility in Drosophila melanogaster: adaptive genetic variations among geographic populations and role of the Y chromosome. *J. Exp. Biol.* **207**, 2735–2743 (2004).

7. R. M. Griffin, D. Le Gall, H. Schielzeth, U. Friberg, Within-population Y-linked genetic variation for lifespan in Drosophila melanogaster. *J. Evol. Biol.* **28**, 1940–1947 (2015).

8. B. A. Payseur, D. C. Presgraves, D. A. Filatov, Introduction: Sex chromosomes and speciation. *Mol. Ecol.* **27**, 3745–3748 (2018).

9. W. R. Rice, Sex Chromosomes and the Evolution of Sexual Dimorphism. *Evolution* **38**, 735–742 (1984).

10. J. A. Coyne, H. A. Orr, "Two rules of speciation" in *Speciation and Its Consequences*, D. Otte, J. A. Endler, Eds. (Sinauer Associates, Inc., 1989), pp. 180–207.

11. H. A. Orr, The population genetics of speciation: the evolution of hybrid incompatibilities. *Genetics* **139**, 1805–1813 (1995).

12. C. I. Wu, *et al.*, Sexual isolation in Drosophila melanogaster: a possible case of incipient speciation. *Proc. Natl. Acad. Sci.* **92**, 2519–2523 (1995).

13. P. Capy, *et al.*, Sexual isolation of genetically differentiated sympatric populations of Drosophila melanogaster in Brazzaville, Congo: the first step towards speciation? *Heredity* **84**, 468 (2000).

14. J. A. Alipaz, C. Wu, T. L. Karr, Gametic incompatibilities between races of Drosophila melanogaster. *Proc. R. Soc. Lond. B Biol. Sci.* **268**, 789–795 (2001).

15. W. R. Rice, B. Holland, The enemies within: intergenomic conflict, interlocus contest evolution (ICE), and the intraspecific Red Queen. *Behav. Ecol. Sociobiol.* **41**, 1–10 (1997).

16. B. Lemos, L. O. Araripe, D. L. Hartl, Polymorphic Y chromosomes harbor cryptic variation with manifold functional consequences. *science* **319**, 91–93 (2008).

17. G. Arnqvist, L. Rowe, *Sexual Conflict* (Princeton University Press, 2005).

18. L. Van Valen, The red queen. *Am. Nat.* **111**, 809–810 (1977).

19. G. A. Parker, "Sexual selection and sexual conflict" in *Sexual Selection and Reproductive Competition in Insects*, (Academic Press, 1979), pp. 123–166.

20. M. F. Camus, J. B. W. Wolf, E. H. Morrow, D. K. Dowling, Single Nucleotides in the mtDNA Sequence Modify Mitochondrial Molecular Function and Are Associated with Sex-Specific Effects on Fertility and Aging. *Curr. Biol.* **25**, 2717–2722 (2015).

21. S. Pitnick, Male size influences mate fecundity and remating interval in Drosophila melanogaster. *Anim. Behav.* **41**, 735–745 (1991).

22. L. Partridge, M. Farquhar, Lifetime mating success of male fruitflies (Drosophila melanogaster) is related to their size. *Anim. Behav.* **31**, 871–877 (1983).

23. D. C. Presgraves, Sex chromosomes and speciation in Drosophila. *Trends Genet.* **24**, 336–343 (2008).

24. M. Kimura, The role of compensatory neutral mutations in molecular evolution. *J. Genet.* **64**, 7 (1985).

25. D. M. Weinreich, L. Chao, Rapid Evolutionary Escape by Large Populations from Local Fitness Peaks Is Likely in Nature. *Evolution* **59**, 1175–1182 (2005).

26. J. A. Ågren, M. Munasinghe, A. G. Clark, Sexual conflict through mother's curse and father's curse. *Theor. Popul. Biol.* (2019) https:/doi.org/10.1016/j.tpb.2018.12.007 (September 10, 2019).

27. D. Arbuthnott, E. M. Dutton, A. F. Agrawal, H. D. Rundle, The ecology of sexual conflict: ecologically dependent parallel evolution of male harm and female resistance in Drosophila melanogaster. *Ecol. Lett.* **17**, 221–228 (2014).

28. W. R. Rice, *et al.*, Inter-locus antagonistic coevolution as an engine of speciation: Assessment with hemiclonal analysis. *Proc. Natl. Acad. Sci.* **102**, 6527–6534 (2005).

29. P. Jensen, *et al.*, Inbreeding effects on standard metabolic rate investigated at cold, benign and hot temperatures in Drosophila melanogaster. *J. Insect Physiol.* **62**, 11–20 (2014).

30. R Core Team, *R: A language and environment for statistical computing. R Foundation for Statistical Computing, Vienna, Austria. URL https://www.R-project.org/* (2018).

31. D. Bates, M. Maechler, B. Bolker, S. Walker, Fitting Linear Mixed-Effects Models Using lme4 | Bates | Journal of Statistical Software. *J. Stat. Softw.* **67**, 1–48 (2015).

32. T. Hothorn, *et al.*, *multcomp: Simultaneous Inference in General Parametric Models* (2017) (October 27, 2018).

33. F. García-González, L. W. Simmons, The evolution of polyandry: intrinsic sire effects contribute to embryo viability. *J. Evol. Biol.* **18**, 1097–1103 (2005).

34. T. Connallon, F. M. Camus, E. H. Morrow, D. K. Dowling, Coadaptation of mitochondrial and nuclear genes, and the cost of mother's curse. *Proc. R. Soc. B Biol. Sci.* **285**, 20172257 (2018).

35. S. P. Otto, T. Day, *A Biologist's Guide to Mathematical Modeling in Ecology and Evolution* (Princeton University Press, 2007).

Table 1: Fitness expressions for the Y-linked locus (**Y**) influencing male siring success, and the viability of offspring resulting from all possible combinations of parental genotypes at **Y** and the compensatory locus **A** (or **X**).

Male Fitness

Male **Y** genotype	Mating success
Y	1
y	$1 + s_m$

Offspring viability

	Mother's Genotype		
Father's **Y** genotype	AA, XX	Aa, Xx	aa, xx
Y	1	$1 - h_c s_c$	$1 - s_c$
y	$1 - s_o$	$1 - h_o s_o$	1

Note: Subscripts for the offspring fitness expressions indicate ...

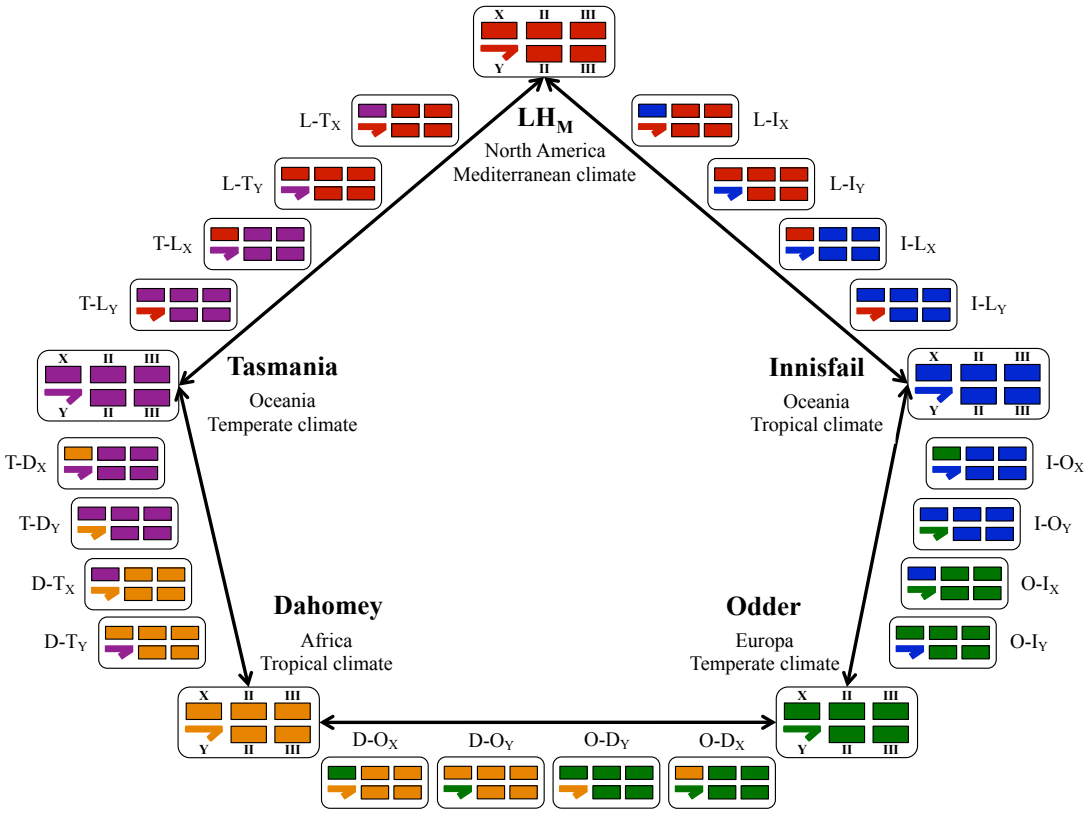

Fig. 1: Schematic of the round robin experimental cross design. Each of the five wild-type populations is color-coded: LH$_M$ (L, red), *Innisfail* (I, blue), *Odder* (O, green), *Dahomey* (D, orange), and *Tasmania* (T, purple). We crossed each wild-type population (large boxes) with two others from either a different continent or climate. This procedure generated four novel genotypes from each cross, so that every combination of the novel sex chromosome pairs experienced a different autosomal genetic background. In total, 10 *Novel X* and 10 *Novel Y* genotypes were generated (small boxes). Coloured bars represent the two major chromosomes (II and III) and chromosome X, with chromosome Y depicted by a half arrow. *Novel* genotypes are annotated as 'genetic background – origin of sex chromosome', with the novel sex chromosome indicated by a X or Y subscript.

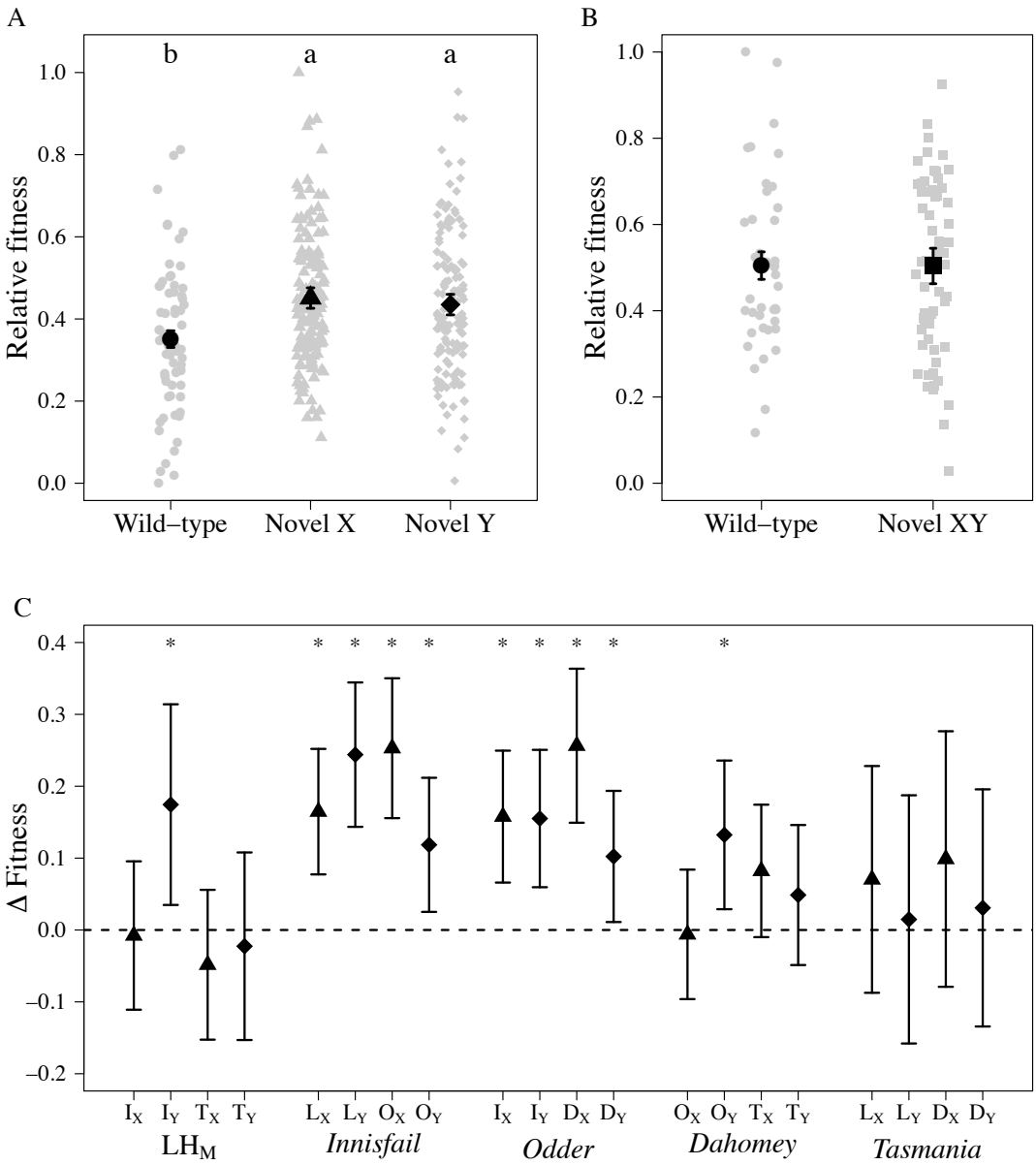

Fig. 2: Male reproductive fitness assays at generation 0. (A) Relative reproductive fitness for *wt* (circles), *novel X* (triangle), and *novel Y* (diamonds) males. We detected statistically significant (P = 2.45e^{-04}) increases in reproductive fitness for both *novel X* and *novel Y* males relative compared to the wild-type populations (Tukey HSD; $P < 0.05$). Mean (±SE) of fitted values from the linear model. The raw data is plotted as grey points. (B) Relative reproductive fitness for *wt* (circles) and *novel XY* (squares) treatment groups. There was no significant difference between *wt* and *novel XY*. Mean (±SE) of fitted values from the linear model. The raw data is plotted as grey points. (C) Change in relative fitness between the *wt* and the *novel* populations. ΔFitness = $\omega_{\text{novel population}}$ - $\omega_{\text{wild-type}}$ with bars indicating bootstrap 95% confidence (see **Materials and Methods**). 10 out of 20 novel populations (*Novel X*: triangle, *novel Y*: diamond) had significantly higher fitness than their *wt* counterpart (indicate by asterisks), and 16 populations had changed in a positive direction, which was more than expected by chance (P = 0.01). Each of the five *wild-type*s are indicated underneath their four novel populations. Capital letters indicate which population the novel sex chromosome originates from (D: *Dahomey*, I: *Innisfail*, L: LH_M, O: *Odder*, and T: *Tasmania*) and the novel sex chromosome is denoted by X or Y subscripts.

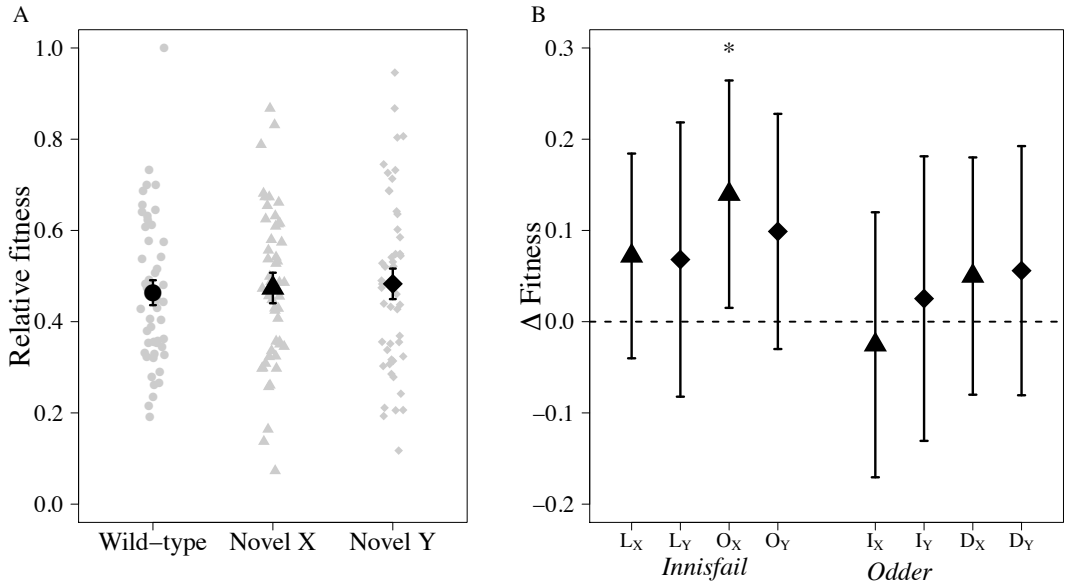

576
577 **Fig. 3:** Reproductive fitness assays at generation 25. We selected 8 of the 10 significant populations for the
578 evolution experiment. (A) Relative reproductive fitness for *wt* (black circle), *novel X* (triangle)**,** and *novel Y*
579 (diamonds) males. *Novel* treatment males no longer had a higher fitness relative to *wt* males after 25 generations of
580 experimental evolution. Mean (±SE) of fitted values from the linear model. The raw data is plotted as grey points.
581 (B) Change in relative fitness between *wt* and *novel X* (triangles) and *novel Y* (diamonds) populations (ΔFitness =
582 $\omega_{\text{novel population}} - \omega_{\text{wild-type}}$), with bootstrap 95% confidence intervals (see **Materials and Methods**). The asterisk
583 indicates whether ΔFitness was significantly greater than zero (Tukey HSD; $P < 0.05$). Each of the *wt* populations
584 are indicated underneath their four *novel* populations. Capital letters indicate which population the novel sex
585 chromosome originates from (D: *Dahomey*, I: *Innisfail*, L: LH_M, O: *Odder*) and the novel sex chromosome is
586 denoted by X or Y subscripts.

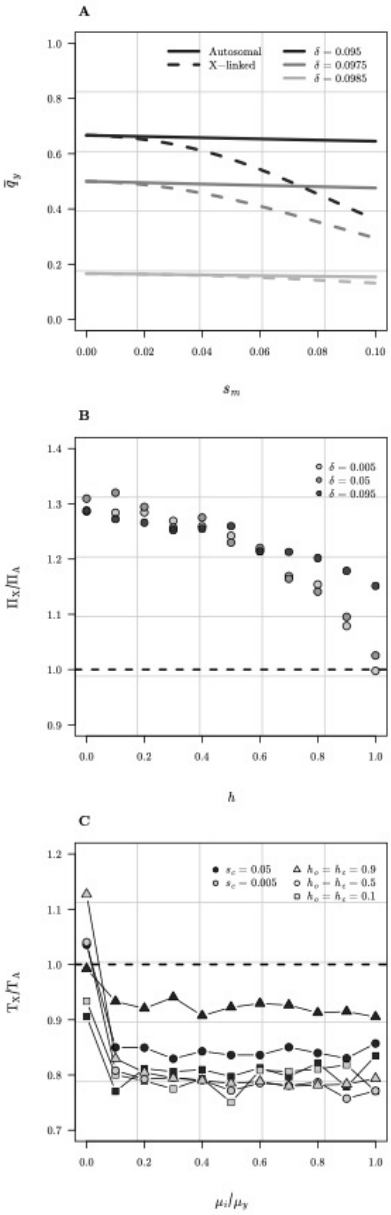

Fig. 4: Summary of theoretical results. (A) Threshold frequencies of the mutant y chromosome at which a new compensatory mutation will experience positive selection for the Autosomal ($\tilde{\boldsymbol{q}}_{\boldsymbol{y}}^{\boldsymbol{A}}$, solid lines) and X-linked ($\tilde{\boldsymbol{q}}_{\boldsymbol{y}}^{\boldsymbol{X}}$, dashed lines) models respectively). As the mutant y chromosome sweeps to fixation, X-linked compensatory mutations will become selectively favoured earlier than autosomal ones. Results are shown for the case of additive fitness ($h_o = h_c = 1/2$), $s_m = 0.1$, and $s_c = 0.005$. (B) The relative probability of invasion for new Autosomal and X-linked compensatory mutations into populations initially fixed for the mutant y chromosome is always greater than or equal to 1, suggesting that when compensatory evolution is limited by mutational variation, the probability of invasion will be higher for X-linked compensatory mutations except under complete dominance. For simplicity we assumed equal dominance for compensatory fitness effects (i.e., $h = h_o = h_c$). Results are shown for three different values of δ (recall that $\delta = s_m - s_o$), where $N = 1{,}000$, $s_m = 0.1$, and $s_c = 0.005$. Each point indicates the mean of 10^6 replicate Wright-Fisher simulations for $\delta = 0.005$ and $\delta = 0.05$, but 5.0×10^6 for $\delta = 0.095$. (C) The relative time to complete a co-evolutionary cycle for the Autosomal vs. X-linked models plotted as a function of the relative mutation rates at the compensatory and Y-linked loci. To explore the consequences of slow vs. fast compensatory dynamics, μ_Y was held constant at 10^{-3}, while μ_i (where $i \in \{\boldsymbol{A}, \boldsymbol{X}\}$) was incremented from 10^{-7} to μ_Y. At low values of μ_i/μ_Y, the rate of compensatory evolution is limited by mutational variation, but at intermediate to high values, the mutant y chromosome and compensatory mutations are more likely to segregate simultaneously. Results are shown for two different 'costs of compensation' (s_c) and three different dominance scenarios (we again assume equal dominance, $h_o = h_c$), and population size $N = 1{,}000$.